

# Optical studies of ZnO/Ag nanojunctions

Shashikant Patole · M. Islam · R. C. Aiyer ·  
Shailaja Mahamuni

Received: 22 July 2005 / Accepted: 31 October 2005 / Published online: 20 June 2006  
© Springer Science+Business Media, LLC 2006

**Abstract** Ag/ZnO nano-hetero-junctions were synthesized by an electrochemical route. The optical absorption spectroscopy and photoluminescence studies reveal the reaction mechanism at the junction. Optical absorption spectra indicate presence of well-defined ZnO excitonic feature along with the Ag surface plasmon absorption feature at 400 nm. Moreover, ZnO green photoluminescence appears on junction formation with Ag. Detailed analysis of emission and excitation processes indicate that efficient charge transfer is taking place from ZnO to Ag. Ag is also responsible for creation of levels in the HOMO-LUMO gap of ZnO. This finding may be of relevance so far as p-type doping in ZnO is concerned.

## Introduction

Free standing quantum dots are often studied using non-contact methods such as optical techniques. Quantum dots are anticipated to be potential candidates for use in a variety of linear and non-linear optical devices. Recently published reports reveal the immediate use of the nanoparticles in catalysis, solar energy conversion, and environmental sciences. The metal/semiconductor nanojunctions are being extensively studied [1–7] for these purposes. Charge transfer between metal and semiconductor under equilibrium condition, is important for its possible use as catalysts as well as non-linear optical

materials. Interaction between ZnO and Ag is also of relevance for realization of p-type ZnO. Nanosize ZnO exhibits a distinct exciton band in the absorption spectra. Excess electrons in the conduction band, however, causes bleaching of the exciton band [1]. Concomitantly, excess conduction electrons in ZnO are also responsible [1–3] for quenching of the defect green luminescence. Therefore ZnO can be used as a model material to investigate the interaction of metal nanoparticles with semiconductor quantum dots by optical probes.

Here we report the investigations on ZnO nanoparticles that show dominantly band gap luminescence. The prime objective of the present work is to understand the interaction at the junction between Ag and ZnO nanoparticles. ZnO nanoclusters used in the present investigations are well passivated and have minimum defects. Optical absorption, photoluminescence (PL) and photoluminescence excitation spectroscopy (PLE) were employed.

## Experimental

Ag/ZnO nanoparticles were synthesized at room temperature, using an electrochemical route [8–10]. The electrochemical bath consisted of acetonitrile and tetrahydrofuran, and the capping agent tetraoctylammonium bromide (TOAB). Silver and zinc foils served as sacrificing anodes while platinum foil served as the cathode. Constant current was passed through the cell in nitrogen atmosphere in order to obtain Ag, ZnO and Ag/ZnO nanoparticles. Ag/ZnO nanoclusters were prepared by two different methods. In case of Ag/ZnO-I, current was passed through Ag prior to that of Zn electrode in the same electrochemical cell. In the other case, Ag and ZnO nanoparticles were synthesized separately. The colloidal solution of Ag and ZnO were

S. Patole · M. Islam · R. C. Aiyer · S. Mahamuni (✉)  
Department of Physics, University of Pune, Pune, India 411 007  
e-mail: shailaja@physics.unipune.ernet.in

mixed and thoroughly stirred to obtain Ag/ZnO-II samples. It may be noted here that, passing current through Zn electrode prior to that of Ag give same results as that of Ag/ZnO-I.

X-ray diffraction (XRD) analysis was carried out on a Philips PW 1840 powder X-ray diffractometer, with  $\text{CuK}_\alpha$  (1.54 Å) as the incident radiation. Transmission electron microscopic (TEM) measurements of drop-coated films were performed on a Philips CN200 microscope operated at an accelerating voltage of 200 kV with resolution of 0.23 nm. Optical absorption spectra of the Ag/ZnO nanoparticle solution were recorded on a Hitachi 330 dual beam spectrophotometer. Photoluminescence (PL) spectra of the Ag/ZnO nanoparticles solution were recorded on a Shimadzu RF-5301PC spectrofluorometer. Drop-coated films of the Ag/ZnO nanoparticles on Si (111) substrates were analyzed by electron dispersive spectroscopy (EDS) on JEOL model JSM-6360A. Infrared absorption spectra were collected using a Shimadzu FTIR-8400 spectrometer.

## Results and discussion

The Ag/ZnO nanoparticles were characterized using XRD for phase and size analysis. Figure 1a depicts the X-ray diffraction pattern of Ag nanocrystals for comparison. Figure 1b shows XRD patterns of Ag/ZnO-I nanocrystals (prepared by passing current through Ag electrode followed to that of Zn). Diffraction pattern clearly reveals Ag (111), (200) along with ZnO (100), (002), (101), (102) confirming fcc and hexagonal structure for Ag and ZnO, respectively [11]. Inter-planar distance for Ag in Ag/ZnO-I is slightly less (2.8%) as compared with pure Ag and the reported JCPD data for Ag. This is a clear indication of substantial interfacial reaction between Ag and ZnO. Average nanocrystal

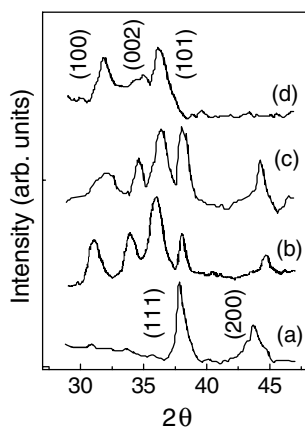


**Fig. 1** X-ray diffraction pattern of (a) Ag nanoparticles, (b) coupled Ag/ZnO-I nanojunctions, (c) Ag/ZnO-II nanoparticles, and (d) ZnO nanoparticles

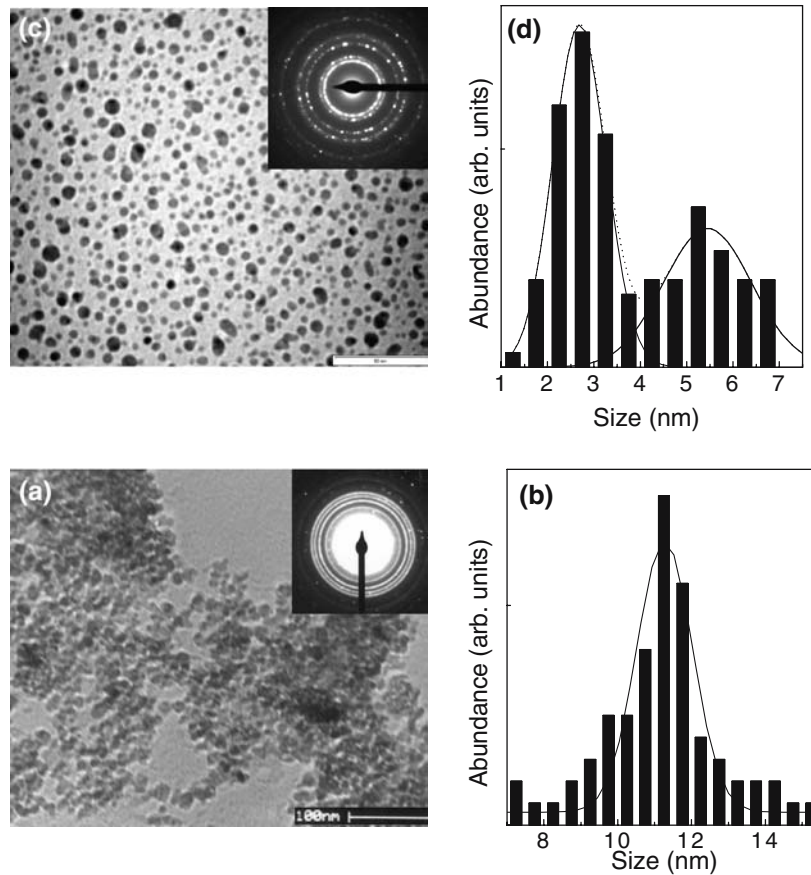
diameter, as estimated by Scherrer formula [12] was about 12.2 nm for Ag nanoparticles and 6.3 nm for ZnO nanocrystals. Figure 1c illustrates XRD of Ag/ZnO-II nanoclusters. XRD pattern is almost same as that of Ag/ZnO-I (Fig. 1b). XRD pattern of ZnO nanoclusters is depicted in Fig. 1d for comparison.

Figure 2a reveals the TEM photographs of Ag/ZnO-I nanostructures. The average size of Ag/ZnO nanocrystal is 11.5 nm. Ag and ZnO particles are not seen separately in TEM photographs. Selective area diffraction pattern shows (Fig. 2a inset) the (100), (002), (101) planes of ZnO nanocrystals and (111), (200) planes of Ag nanocrystals. The electron diffraction pattern confirms presence of Ag and ZnO. TEM analysis of pure Ag nanoparticles synthesized under similar conditions show size of about 5.5 nm. The higher size obtained in XRD is thus indicative of agglomeration of nanoparticles while forming dense film suitable for analysis. The transmission electron micrograph of Ag/ZnO-II reveals (Fig. 2c) separately dispersed 3 nm ZnO nanoparticles and 5.5 nm Ag particles. The capping agent is not seen in TEM micrograph as separate shell because of its organic nature [10]. EDS analysis indicate presence of Ag, Zn, and O which confirms the purity of the samples.

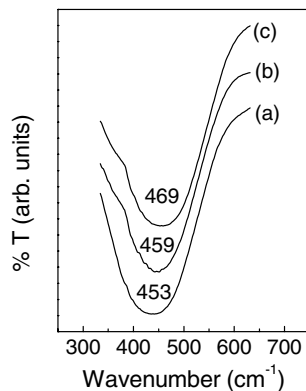
The FTIR spectrum of stretching mode in pure ZnO, Ag/ZnO-I, and Ag/ZnO-II nanoparticles are shown in Fig. 3. A peak at  $453\text{ cm}^{-1}$  is a distinct stretching mode of ZnO [13]. In the case of Ag/ZnO-II the peak is observed at  $459\text{ cm}^{-1}$  and for coupled Ag/ZnO-I the peak is observed at  $469\text{ cm}^{-1}$ . The shift in the stretching mode of ZnO could be due to substantial interaction between ZnO and Ag. The shift in Ag/ZnO-II is less compared to Ag/ZnO-I.

Figure 4a–c, and d display the optical absorption spectra of Ag, Ag/ZnO-I, Ag/ZnO-II, and ZnO nanocrystals, respectively. Two distinct peaks at about 345 nm and 400 nm are clearly revealed for Ag/ZnO-I and Ag/ZnO-II. The absorption peak at 345 nm is the excitonic absorption of ZnO nanocrystal while that located at 400 nm is the surface plasmon (SP) resonance absorption band of Ag [14]. Excitonic absorption peak [15] is blue shifted with respect to bulk absorption, which appears at 3.34 eV (371 nm) at room temperature. The composite formation primarily affects the SP band of metal depending upon the dielectric constant of the oxide semiconductor [16] as well as electron density in metal particle. In the present case, core/shell of nanocrystalline Ag and ZnO is not forming. Core/shell (Ag/ZnO) formation can be seen from the modulated optical absorption of Ag [2]. The observation of distinct features of ZnO and Ag in optical absorption spectra as well as TEM studies, discard the possibility of formation of core/shell nanostructure. Subsequently, we believe that coupled Ag/ZnO nanoparticles must have formed.

**Fig. 2** (a) Transmission electron micrograph of coupled Ag/ZnO-I nanojunctions, (b) histogram showing particle size distribution of coupled Ag/ZnO-I nanostructure, (c) Transmission electron micrograph of Ag/ZnO-II nanoparticles, and (d) histogram showing particle size distribution. Inset shows selective area electron diffraction pattern



ZnO absorption spectra reveal sharper excitonic feature in Ag/ZnO (coupled phase) at about 345 nm. Bleaching of the excitonic feature due to accumulation of electrons in conduction band of ZnO is well established [1–3]. In the present case, excitonic feature is getting sharper on coupling with Ag nanoparticles. Substantial charge transfer from ZnO LUMO orbitals to Ag nanoparticles should be responsible for peculiar optical absorption feature. Ag SP absorption feature remains at about 400 nm.



**Fig. 3** FTIR spectrum of stretching mode in (a) ZnO nanoparticles, (b) Ag/ZnO-II nanoparticles (c) coupled Ag/ZnO-I nanojunctions

PL emission spectra of nano-sized Ag and ZnO are compared with Ag/ZnO nano-junctions. Ag/ZnO nano-structures are produced by various different ways. (a) Current through Ag was passed prior to that of Zn electrode to yield Ag/ZnO (b) Current through Zn electrode was passed prior to that of Ag (c) Current through Ag and Zn was passed simultaneously. However, all these experiments yield the similar nanoparticles. It is worthwhile to note here that in case of Ag/Au bimetallic nanoparticles [9], variation

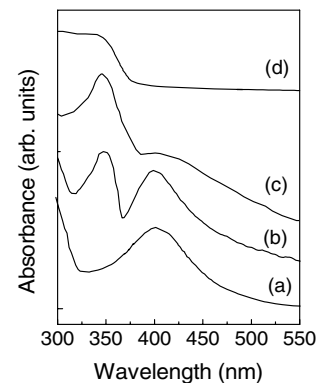


**Fig. 4** Optical absorption spectra of (a) Ag nanoparticles, (b) coupled Ag/ZnO-I nanojunctions, (c) Ag/ZnO-II nanoparticles, and (d) ZnO nanoparticles

in process conditions drastically altered the nanostructure configuration. Figure 5a–c, and d exhibit PL emission spectra of Ag, Ag/ZnO-I, Ag/ZnO-II, and ZnO respectively. While Fig. 6a–c, shows PLE spectra recorded (at emission wavelength of 470 nm) to examine the influence of junction formation on Ag luminescence.

Pure Ag nanoparticles of size about 9 nm show PL emission at 480 nm (as seen in Fig. 5a) when excited at 320 nm. Corresponding PL excitation spectra depict broad feature at 355 nm (Fig. 6a). Luminescence from Ag nanoparticles is observed due to inter-band transitions as well as from re-radiation due to surface plasmons [17, 18]. Inter-band transition of Ag is located at about 310 nm while SP resonance occurs around 358 nm [19]. Surface defects often play a vital role in PL emission of nanoparticles. Metal surfaces and nanoparticles show remarkably weak luminescence [20, 21] as compared to semiconductor nanoparticles. Moreover, PL emission wavelength is almost always red shifted with respect to the absorption wavelength [22]. Under such conditions, we compare PL excitation wavelength of nanoparticles with PL emission from metal surfaces.

Subsequently, PLE feature of Ag nanoparticles at 355 nm is attributed to radiative decay of surface plasmons. Ag/ZnO nanoparticles obtained by all the above mentioned methods display PL emission at 370, 470 and 540 nm (Fig. 5b). Emission features at 370 nm and at 540 nm are due to excitonic recombination and defect luminescence in ZnO, respectively [9, 23]. Defect luminescence at 540 nm arises in Ag/ZnO nanostructures at the expense of ZnO excitonic recombination feature. Features at 470 nm and 540 nm are inherently broad.

Present PL data on Ag/ZnO-I is comparable with that of reported [24] PL studies for Ag doped ZnO films. Ag

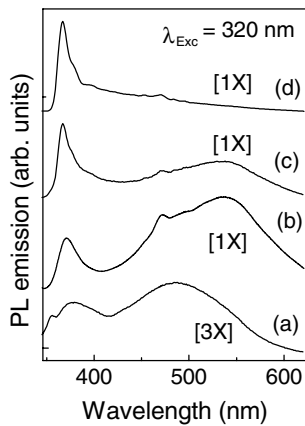


**Fig. 5** Photoluminescence emission spectra of (a) Ag nanoparticles, (b) coupled Ag/ZnO-I nanojunctions, (c) Ag/ZnO-II nanoparticles, and (d) ZnO nanoparticles. Square bracket indicates the multiplication factor on Y-axis.  $\lambda_{exc} = 320$  nm

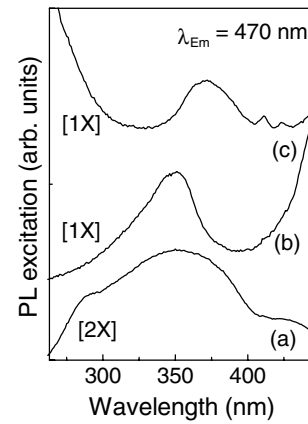


**Fig. 6** Photoluminescence excitation spectra of (a) Ag nanoparticles, (b) coupled Ag/ZnO-I nanojunctions, (c) Ag/ZnO-II nanoparticles, recorded at emission wavelength  $\lambda_{em} = 470$  nm. Square bracket indicates the multiplication factor on Y-axis

doping is responsible for two distinct bands located at 2.29 and 2.50 eV. It was proposed that yellow/green band could have diminished intensity in Ag/ZnO due to the occupation of Ag at Zn vacancies. Ag related defect level is also observable at about 2.50 eV. In the present case, we observed a new feature at about 2.63 eV in Ag/ZnO-I. In short, PL data clearly indicate substantial interfacial reaction in Ag and ZnO. Or in other words, interface comprises of Ag doped ZnO layer.

Figure 6b shows PL excitation recorded at fixed emission of 470 nm. A hump like feature at 353 nm is seen in PLE for Ag/ZnO-I nanoclusters. The feature is almost at the same wavelength as that of the pure Ag nanoparticles. In case of Ag/ZnO-II, the PLE feature is slightly red-shifted (Fig. 6c) and appears at about 370 nm. In fact, SP resonance absorption as well as PL emission feature of silver are weak in this sample. Moreover, the signal is

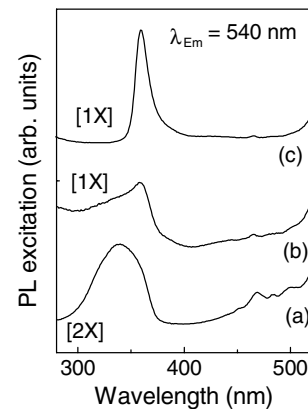


**Fig. 7** Photoluminescence excitation spectra of (a) coupled Ag/ZnO-I nanojunctions, (b) Ag/ZnO-II nanoparticles, and (c) ZnO nanoparticles, recorded at emission wavelength  $\lambda_{em} = 540$  nm. Square bracket indicates the multiplication factor on Y-axis

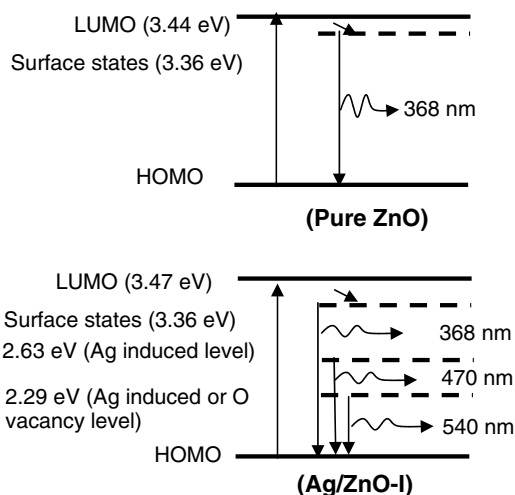
predominantly due to ZnO. Subsequently, PLE recorded at emission wavelength of 470 nm could be most probably due to ZnO.

Figure 7 compares PLE features measured at emission wavelength of 540 nm (essentially, to study the effect of junction formation on ZnO quantum dots). PLE spectra of Ag/ZnO-I reveal rather broad feature at 342 nm. While, in case of Ag/ZnO-II, PL excitation recorded at the emission wavelength of 540 nm appears at about 360 nm (Fig. 7b), which resembles to that for pure ZnO nanocrystals (Fig. 7c). This is a clear indication of substantial interaction between ZnO and Ag in the coupled nanoparticles viz. Ag/ZnO-I while minimal interaction in case of Ag/ZnO-II. In fact substantial broad PLE feature can be fitted with two peaks, one corresponding to pure ZnO and higher energy feature which could have origin due to Ag. Pure ZnO nanoparticles (size 5 nm) show PL at about 367 nm when excited at 320 nm as seen from Fig. 5d. Green defect luminescence is strongly quenched in this case. Detailed studies of ZnO nanoparticles are reported elsewhere [9, 23].

PL emission of Ag/ZnO-II nanoparticles as depicted in Fig. 5c, indicate subtle interaction between Ag and ZnO. PL excitation spectra (Fig. 6c) of the same sample recorded at emission wavelength of 470 nm is quite similar to that of the pure Ag nanoparticles. PL excitation spectra at emission wavelength of 540 nm, show (Fig. 7c) hump like feature at 360 nm revealing weak interaction between ZnO and Ag. Accumulation of electrons in ZnO results [1] in the quenching of green luminescence and bleaching of excitonic feature. In the present case, green luminescence is increasing at the cost of excitonic luminescence. Along with it, the PLE feature ( $\lambda_{em} = 540$  nm) is concurrently getting broader indicating the appearance of the shallow levels near the band edge. Pure ZnO quantum dots show strongly quenched visible luminescence although a sharp PLE feature is seen at about 367 nm when emission was kept constant at 540 nm. In Ag/ZnO-I (coupled system), PLE feature becomes asymmetrical and broad. Visible luminescence gets quite strong at 540 nm and is also associated with Ag defect level related feature at 480 nm. Evolution of schematic energy level diagram for Ag/ZnO-I is given in Fig. 8.

## Conclusions

In summary, coupled Ag/ZnO quantum dots were obtained with the aid of electrochemical route. XRD, optical absorption measurements, and TEM studies support formation of coupled nano-junctions and also indicate effective charge transfer from ZnO to Ag. The green



**Fig. 8** Schematic electron energy level diagram in pure ZnO and Ag/ZnO-I nanojunction

photoluminescence emission feature becomes dominant due to coupling of ZnO nanoparticles with Ag. PLE recorded at emission wavelength of 540 nm, for Ag/ZnO-I reveal blue shifted, broad feature at about 342 nm indicating substantial change in the electron energy levels while that of Ag/ZnO-II, show rather broad feature at 360 nm indicating appearance of shallow levels in ZnO. PLE data as well as appearance of a new feature at about 470 nm in Ag/ZnO-I indicates formation of Ag doped ZnO interface.

**Acknowledgements** We thank K.C. Rustagi for helpful and encouraging discussions. We also thank V.V. Nikesh for help in the experimental work. Financial support by Council of Scientific and Industrial Research, New Delhi is gratefully acknowledged.

## References

1. Subramanian V, Wolf EE, Kamat PV (2003) *J Phys Chem B* 107:7479
2. Hirakawa T, Kamat PV (2004) *Langmuir* 20:5645
3. Wood A, Giersig M, Mulvaney P (2001) *J Phys Chem B* 105:8810
4. Chen S, Nickel U (1996) *J Chem Soc Faraday Trans* 92:1555
5. Chen S, Nickel U (1996) *Chem Commun* 133
6. Ballesteros JM, Solis J, Serna R, Alonso CN (1999) *Appl Phys Lett* 74:2791
7. Ma GH, He J, Rajiv K, Tang SH, Yang Y, Nogami M (2004) *Appl Phys Lett* 84:4084
8. Mahamuni S, Borgohain K, Bendre BS, Leppert VJ, Risbud SH (1999) *J Appl Phys* 85:2861
9. Isalm M, Patole S, Aiyer RC and Mahamuni S (to be published)
10. Reetz MT, Helbig WJ (1994) *J Am Chem Soc* 116:7401
11. Powder diffraction files (1984) JCPD, p. 783, 663
12. Cullity BD, Stock SR (2001) *Elements of X-ray diffraction*. Prentice Hall, Upper Saddle, NJ
13. Wang Z, Zhang H, Zhang L, Yuan J, Yan S, Wang C (2003) *Nanotechnology* 14:11

14. Taleb A, Petit C, Pileni MP (1998) *J Phys Chem B* 102:2214
15. Liang Y, Yoffe AD (1968) *Phy Rev Lett* 20:59
16. Hovel H, Fritz S, Hilger A, Kreibig U, Vollmer M (1993) *Phys Rev B* 48:18178
17. Boyd GT, Yu ZH, Shen YR (1986) *Phy Rev B* 33:7923
18. Lee KC (1985) *Surf Sci* 163:L759
19. Andersen PC, Jacobson ML, Rowien KL (2004) *J Phys Chem B* 108:2148
20. Wilcoxon JP, Martin JE, Parsapour F, Wiedenman B, Kelley D (1998) *J Chem Phys* 108:9137
21. Mooradian A (1969) *Phys Rev Lett* 22:185
22. Nikesh VV, Mahamuni S (2001) *Semicond Sci Technol* 16:687 and references therein
23. Bendre BS, Mahamuni S (2004) *J Mat Res* 19:737
24. Lee HY, Ko HJ, Yao T (2003) *Appl Phys Lett* 82:523